Cavendish-HEP-95/05
hep-ph/9509353
September 1995

Studies of Unitarity at Small x Using the Dipole Formulation*

G.P. Salam

Cavendish Laboratory, Cambridge University,
Madingley Road, Cambridge CB3 0HE, UK

e-mail: salam@hep.phy.cam.ac.uk

Abstract

Mueller's dipole formulation of onium-onium scattering is used to study unitarity corrections to the BFKL power growth at high energies. After a short discussion of the spatial distribution of colour dipoles in a heavy quarkonium and the associated fluctuations, results are presented showing that the one and two-pomeron contributions to the total cross section are the same at a rapidity $Y \simeq 14$. Above this rapidity the large fluctuations in the onium wave function cause the multiple pomeron series to diverge. Resumming the series allows one to show that unitarity corrections set in gradually for the total cross section, which is dominated by rare, large, configurations of the onia. The elastic cross section comes mostly from much smaller impact parameters and has significant unitarity corrections starting at a rapidity $Y \simeq 8$.

*Research supported by the UK Particle Physics and Astronomy Research Council

1 Introduction

The BFKL pomeron [1, 2, 3] causes the amplitudes for certain high energy processes, which are also hard processes, to rise as a power of the centre of mass energy. At very high energies this rapid rise will cause the amplitudes to violate unitarity. Unitarity is the statement that for any given initial states and impact parameter, the probability of interaction cannot be larger than one. Because it is a limit on the interaction for each impact parameter, one cannot tell when an amplitude violates unitarity without knowing how the amplitude is distributed in impact parameter. This has also been one of the main uncertainties in calculations (for example [4]) of the shadowing corrections to BFKL evolution using the GLR equation [5]. However knowledge of the average interaction for a given impact parameter is insufficient. The wave functions for each of the colliding objects consist of a variety of states each with some amplitude. What can happen is that for a given impact parameter the average interaction can be dominated by occasional rare combinations of states which have a large interaction and therefore large unitarity corrections. However because these configurations are rare, the average interaction can still be small and one can be misled into thinking that there should be no unitarity corrections.

One of the simplest frameworks in which to study the BFKL pomeron, and the onset of unitarity corrections, is the dipole formulation, proposed by Mueller [6, 7, 8, 9]. For sufficiently heavy onia, α_S, the strong coupling constant, is small and one can apply perturbation theory. One starts with a $q\bar{q}$ state and considers the correction to the wave function which comes from adding one gluon, causing the initial $q\bar{q}$ colour dipole to branch into two colour dipoles (qg and $g\bar{q}$). In the small-x, leading N_C approximation, each of these dipoles can then branch again, independently, and the process repeats itself, building up a cascade of colour dipoles. One can then calculate the onium-onium elastic amplitude from the interactions between the dipoles of the two onia. The lowest order interaction is the exchange of a colour neutral pair of gluons. This is one pomeron exchange. Exchange of larger numbers of pairs of gluons corresponds to multiple pomeron exchange. This approach is particularly suited to the study of unitarity because it is formulated in impact parameter and also because it contains all the information on the fluctuations in the onium configurations. Further, because the onium wave functions are each evolved to only half the total rapidity, unitarity corrections to the cross section should set in long before the density of partons rises to the point where corrections to the wave functions need also be taken into account, i.e. long before the wave functions saturate.

In this paper, a Monte Carlo simulation will be used to calculate the full, unitarised, amplitude for high energy onium-onium elastic scattering. Section 2 gives a brief review

of the dipole formalism. Section 3 discusses certain properties of the onium wave function, showing that the distribution of dipoles is more central than had been suggested in [8], and giving more information on the exponential tails of the fluctuations in dipole density, which were first mentioned in [10]. These fluctuations have as a consequence that the k-pomeron series is divergent, though it can be resummed by interchanging the order of the summations over k and over configurations of the onia [8]. This and other consequences of fluctuations are illustrated in section 4, where the main results of the paper are presented: the k-pomeron and unitarised amplitudes for onium-onium scattering, as a function of rapidity. One and two pomeron contributions to the total cross section are seen to be equal at a rapidity of 14, but the unitarised total cross section carries on growing well beyond this point. The elastic cross section has much stronger unitarity corrections and the behaviour of the power of the growth of the unitarised and 1-pomeron elastic cross sections differ significantly above $Y = 8$.

2 Onium-onium scattering

2.1 Single pomeron exchange

The amplitude for exchange of a single pomeron between two onia moving fast in opposite directions, with a centre-of-mass energy $\sqrt{s}$ is:

$$A(\mathbf{r}, Y) = -i \int \mathrm{d}^2\mathbf{b}\mathrm{d}^2\mathbf{b}' \int \mathrm{d}z\mathrm{d}z' \Phi(\mathbf{b}, z)\Phi(\mathbf{b}', z')F(\mathbf{b}, \mathbf{b}', \mathbf{r}, Y) \tag{1}$$

The rapidity Y is approximately $\log s/M^2$, with M being the onium mass. The amplitude is determined for a fixed relative impact parameter $\mathbf{r}$ between the onia and $\Phi(\mathbf{b}, z)$ is the square of the heavy quark-antiquark part of the onium wave functions with $\mathbf{b}$ the transverse separation between the quark and antiquark and z the longitudinal momentum fraction of the antiquark. For single pomeron exchange, $F = F^{(1)}$, with

$$F^{(1)}(\mathbf{b}, \mathbf{b}', \mathbf{r}, Y) = -\int \frac{\mathrm{d}^2\mathbf{c}}{2\pi c^2}\frac{\mathrm{d}^2\mathbf{c}'}{2\pi c'^2}\mathrm{d}^2\mathbf{R}\mathrm{d}^2\mathbf{R}' f(\mathbf{R} - \mathbf{R}', \mathbf{c}, \mathbf{c}')n(c, b, R, y)n(c', b', |\mathbf{R}' - \mathbf{r}|, Y - y) \tag{2}$$

The factors $n(c, b, R, y)$ are the density of dipoles of size c at a distance R from a parent onium of size b after evolution through a rapidity y. The terms $1/2\pi c^2$ are just to compensate for the normalisation of each wave function (which from now on refers to the gluon distribution of an onium of fixed size). Note that for one pomeron exchange the division of rapidity between the two onia (the choice of y) is arbitrary. The amplitude (divided by $(-i)$) for interaction between a dipole of size $\mathbf{c}$ and one of size $\mathbf{c}'$ whose centres are separated by $\mathbf{r}$, $f(\mathbf{r}, \mathbf{c}, \mathbf{c}')$, is the following:

$$\int \mathrm{d}^2\mathbf{r}\mathrm{e}^{i\mathbf{q}.\mathbf{r}} f(\mathbf{r},\mathbf{c},\mathbf{c}') = \frac{\alpha_S^2}{2}\int \frac{\mathrm{d}^2\ell}{|\ell|^2|\mathbf{q}-\ell|^2}\left[\mathrm{e}^{i\ell.\mathbf{c}/2}-\mathrm{e}^{-i\ell.\mathbf{c}/2}\right]\left[\mathrm{e}^{-i\ell.\mathbf{c}'/2}-\mathrm{e}^{i\ell.\mathbf{c}'/2}\right]$$
$$\left[\mathrm{e}^{i(\mathbf{q}-\ell).\mathbf{c}/2}-\mathrm{e}^{-i(\mathbf{q}-\ell).\mathbf{c}/2}\right]\left[\mathrm{e}^{-i(\mathbf{q}-\ell).\mathbf{c}'/2}-\mathrm{e}^{i(\mathbf{q}-\ell).\mathbf{c}'/2}\right] \quad (3)$$

This is considered in more detail in the next section. The normalisation is chosen such that the total cross section is:

$$\sigma_{tot}(Y) = 2\int \mathrm{d}^2\mathbf{r}\ \mathrm{Im}A(\mathbf{r},Y) \quad (4)$$

while for the elastic cross section

$$\frac{\mathrm{d}\sigma_{el}}{\mathrm{d}t} = \frac{1}{4\pi}|A(q,Y)|^2, \quad (5)$$

with $t=-q^2$ and

$$A(q,Y) = \int \mathrm{d}^2\mathbf{r}\mathrm{e}^{i\mathbf{q}.\mathbf{r}}A(\mathbf{r},Y). \quad (6)$$

The term total amplitude will be used to refer to $F(b,b',r,Y)$ integrated over $\mathbf{r}$, which is equal to half the total cross section (ignoring the integral of eq. (1)).

In the limit $r \gg b,b'$, and with $\log r^2/bb' \ll kY$, one has the following expression for $F^{(1)}$

$$F^{(1)}(b,b',r,Y) = -\frac{8\pi\alpha_S^2 bb'}{r^2}\log\left(\frac{16r^2}{bb'}\right)\frac{\exp[(\alpha_{\mathcal{P}}-1)Y-\log^2(16r^2/bb')/kY]}{(\pi ky)^{3/2}}, \quad (7)$$

where $(\alpha_{\mathcal{P}}-1) = 4\log 2\alpha_S N_C/\pi$ and $k = 14\alpha_S N_C\zeta(3)/\pi$, $\zeta(n)$ being the Riemann zeta function.

It is convenient to work in impact parameter and with this normalisation, because the unitarity condition is then simply $|F(\mathbf{r},Y)| \leq 1$. It is the exponential dependence on Y which causes this condition to be violated as Y increases beyond a certain limit.

2.2 Dipole-Dipole interaction

In [8] the dipole-dipole interaction, $f(r,\mathbf{c},\mathbf{c}')$ was approximated by:

$$f(\mathbf{r},\mathbf{c},\mathbf{c}') = \delta^2(\mathbf{r})\pi\alpha_S^2 c_<^2\left(1+\log\frac{c_>}{c_<}\right) \quad (8)$$

This is correct if one averages over angles and integrates over $\mathbf{r}$, and is therefore perfectly adequate for studying single pomeron exchange. However to study multiple pomeron exchange one needs to know the full expression. It is obtained by performing the inverse Fourier

transform in eq. (3), noting that $f(q)$, the Fourier transform of the potential, is a convolution of two identical terms, each of which gives the single gluon potential between a pair of dipoles. The result is that $f(\mathbf{r})$ is then simply the square of the two-dimensional dipole-dipole potential:

$$f(\mathbf{r},\mathbf{c},\mathbf{c}') = \frac{\alpha_S^2}{2}\left[\log\frac{|\mathbf{r}+\mathbf{c}/2-\mathbf{c}'/2||\mathbf{r}-\mathbf{c}/2+\mathbf{c}'/2|}{|\mathbf{r}+\mathbf{c}/2+\mathbf{c}'/2||\mathbf{r}-\mathbf{c}/2-\mathbf{c}'/2|}\right]^2, \tag{9}$$

as would be expected for the exchange of two gluons between a pair of dipoles in two dimensions.

2.3 Multiple pomeron exchange

To recover the unitarity condition it is necessary to include higher order terms. The ones which will be considered here are k-pomeron exchange. This corresponds to the exchange of k colour neutral pairs of gluons between the two onia. As is discussed in [8] and reviewed here in section 2.4, at rapidities where unitarity effects are setting in, it should be safe to neglect corrections to the wave functions which would arise due to saturation of the wave functions. To evaluate multiple pomeron exchange, it is no longer adequate to use the average dipole distribution: it is necessary to know the higher moments of the wave functions

In [8], the equations governing the evolution of the wave function are expressed using an operator formalism: the operator $a^\dagger(\mathbf{r},\mathbf{b})$ ($d^\dagger(\mathbf{r},\mathbf{b})$) creates a dipole at position $\mathbf{r}$ and with size $\mathbf{b}$, in the right (left) moving onium. The basic vertex of the dipole picture is then V_1:

$$V_1 = \frac{\alpha_S N_C}{2\pi^2}\int \frac{b_{01}^2}{b_{02}^2 b_{12}^2}\mathrm{d}^2\mathbf{b}_{01}\mathrm{d}^2\mathbf{b}_2\mathrm{d}^2\mathbf{r}\, a^\dagger(\mathbf{r}+\frac{\mathbf{b}_{12}}{2},\mathbf{b}_{02})a^\dagger(\mathbf{r}+\frac{\mathbf{b}_{02}}{2},\mathbf{b}_{12})a(\mathbf{r},\mathbf{b}_{01}). \tag{10}$$

This expresses the branching of a colour dipole of size $\mathbf{b}_{01}$ at position $\mathbf{r}$ into the two dipoles which are formed by the production of a gluon at $\mathbf{b}_2$. Together with this there are virtual corrections

$$V_2 = -\frac{\alpha_S N_C}{2\pi^2}\int \frac{b_{01}^2}{b_{02}^2 b_{12}^2}\mathrm{d}^2\mathbf{b}_{01}\mathrm{d}^2\mathbf{b}_2\mathrm{d}^2\mathbf{r}\, a(\mathbf{r},\mathbf{b}_{01})a^\dagger(\mathbf{r},\mathbf{b}_{01}) \tag{11}$$

which ensure the conservation of probability: when a dipole branches into two, the original dipole is lost. For a given dipole, the branching process and the virtual corrections depend only on its size, not on its position or on the other dipoles that are present. The probability of finding a configuration made up of dipoles at positions and sizes $\{\mathbf{r}_1,\mathbf{c}_1;\ldots;\mathbf{r}_n,\mathbf{c}_n\}$ after the evolution through a rapidity y of an initial dipole at $\mathbf{r}_0$ of size $\mathbf{b}=\mathbf{b}_{01}$ is then:

$$P(\{\mathbf{r}_1,\mathbf{c}_1;\ldots;\mathbf{r}_n,\mathbf{c}_n\},\mathbf{r}_0,\mathbf{b},y) = \langle 0|a(\mathbf{r}_1,\mathbf{c}_1)\ldots a(\mathbf{r}_n,\mathbf{c}_n)\mathrm{e}^{yV_R}a^\dagger(\mathbf{r}_0,\mathbf{b})|0\rangle \tag{12}$$

where $V_R = V_1 + V_2$. There is a similar expression for the left-moving onium.

The amplitude $F^{(k)}(\mathbf{r}, Y)$ for the exchange of k pomerons is then, analogously to eq. 2,

$$F^{(k)}(\mathbf{r}, Y) = \langle 0|\mathrm{e}^{a_1+d_1}\frac{(-f)^k}{k!}\mathrm{e}^{yV_L+(Y-y)V_R}d^\dagger(\mathbf{r}+\mathbf{r}_0, \mathbf{b}_L)a^\dagger(\mathbf{r}_0, \mathbf{b}_R)|0\rangle. \tag{13}$$

The term a_1 is

$$a_1 = \int \mathrm{d}^2\mathbf{r}\mathrm{d}^2\mathbf{c}\; a(\mathbf{r}, \mathbf{c}) \tag{14}$$

with an analogous expression for d_1. The operator f gives the sum of all the dipole-dipole interactions occurring for that impact parameter:

$$f = \int \mathrm{d}^2\mathbf{R}\mathrm{d}^2\mathbf{R}'\mathrm{d}^2\mathbf{c}\mathrm{d}^2\mathbf{c}' f(\mathbf{R}-\mathbf{R}', \mathbf{c}, \mathbf{c}')d^\dagger(\mathbf{R}, \mathbf{c})d(\mathbf{R}, \mathbf{c})a^\dagger(\mathbf{R}', \mathbf{c}')a(\mathbf{R}', \mathbf{c}'). \tag{15}$$

Summing together all orders of pomeron exchange, one obtains an expression which explicitly satisfies the unitarity bound: the S-matrix is

$$S(\mathbf{b}, \mathbf{b}', \mathbf{r}, Y) = 1 + F(\mathbf{b}, \mathbf{b}', \mathbf{r}, Y) = \langle 0|\mathrm{e}^{a_1+d_1}\mathrm{e}^{-f}\mathrm{e}^{yV_L+(Y-y)V_R}d^\dagger(\mathbf{r}+\mathbf{r}_0, \mathbf{b})^\dagger(\mathbf{r}_0, \mathbf{b}')|0\rangle. \tag{16}$$

Where it would otherwise be unclear which quantity is being discussed, the unitarised amplitude F will be referred to as $F^{(unit)}$. This can be cast into a form more suitable for use with a Monte Carlo simulation. Let γ be a particular dipole configuration for the left moving onium, which contains dipoles of position and size $(\mathbf{r}_1, \mathbf{c}_1)\ldots(\mathbf{r}_{n_\gamma}, \mathbf{c}_{n_\gamma})$. For an onium at impact parameter $\mathbf{r}$, of size $\mathbf{b}$, and evolved to a rapidity of Y, the probability of finding such a configuration is defined as $P_\gamma(\mathbf{b}, \mathbf{r}, Y)$. In these terms, the S-matrix becomes:

$$S(Y, \mathbf{r}, \mathbf{b}, \mathbf{b}') = \sum_{\gamma,\gamma'} P_\gamma(\mathbf{r}_0, \mathbf{b}, y)P_{\gamma'}(\mathbf{r}_0+\mathbf{r}, \mathbf{b}', Y-y)\exp(-f_{\gamma,\gamma'}). \tag{17}$$

The definition of $f_{\gamma,\gamma'}$ is:

$$f_{\gamma,\gamma'} = \sum_{i=1}^{n_\gamma}\sum_{j=1}^{n_{\gamma'}} f(\mathbf{r}_i - \mathbf{r}'_j, \mathbf{c}_i, \mathbf{c}'_j) \tag{18}$$

With this form for the interaction, the cross section can be obtained by randomly producing the configurations for each onium, and working out $f_{\gamma,\gamma'}$ for each point in impact parameter. This is repeated with many configurations to obtain the average S-matrix. Since $f_{\gamma,\gamma'}$ is always positive, it is obvious from eq. 17 that the unitarity bound is satisfied.

2.4 Division of the rapidity interval

As already mentioned, for one pomeron exchange, the division of the rapidity interval between the two onia is arbitrary. The onium-onium scattering amplitude is independent of y in eq. (2). This is because y is not a physical parameter. For multi-pomeron exchange, though y is still not a physical parameter, it does become a parameter of the approximation, because one is ignoring corrections to wave functions which have been evolved to y and $(Y-y)$ [8]: the fractional correction to the forward amplitude from 2 pomeron exchange is $O(\alpha_S^2 e^{(\alpha_{\mathcal{P}}-1)Y})$. For any given part of the wave function, the leading correction to that part of the wave function is of the order of $O(\alpha_S^2 e^{(\alpha_{\mathcal{P}}-1)y})$ (or $O(\alpha_S^2 e^{(\alpha_{\mathcal{P}}-1)(Y-y)})$ for the other wave function). If one divides the rapidity equally between the two onia, $y = Y/2$, corrections to the wave functions do not become important, in principle, until twice the rapidity where corrections appear in scattering. However if one divides the rapidity interval asymmetrically (e.g. $y \simeq Y$), corrections to the wave function which have been neglected are of the same same order as corrections to scattering amplitude and one will underestimate the total unitarity corrections. This of course ignores any of the details of the impact parameter distribution of the wave function, as well as fluctuations which might cause occasional larger dipole densities, but the basic argument should still be valid.

3 Some properties of the wave function

3.1 Monte Carlo calculation of the wave functions

The first stage in a Monte Carlo calculation of onium-onium scattering is to simulate the branching processes which produce the wave functions of the two onia. For each onium, one starts with an initial dipole of size b and produces a gluon with a random position whose distribution is determined by eq. (10). The rapidity of the gluon is chosen with an exponentially decaying distribution in accordance with the virtual corrections of eq. (11). The procedure is then repeated with the two new dipoles, and then the dipoles they produce, etc., until the rapidity of any new gluons would exceed the rapidity to which one is evolving. The main difficulty in implementing this procedure is that the integrals in eqs. (10) and (11) are divergent for small dipole sizes. This divergence has to be regulated, and the most appropriate method for a Monte Carlo simulation is the introduction of a lower cutoff (c_{low}) on the dipole size. In any observable quantity the divergence cancels out between the real and virtual terms, and the dependence on the cutoff should disappear as it is taken to zero. For a finite cutoff, though, any observable will be somewhat modified. The problem with reducing the cutoff to zero is that the number of dipoles in the wave function is $\propto 1/c_{low}$. When considering

onium-onium collisions the time taken to calculate an amplitude is the proportional to the product of the number of dipoles in each onium, and so is $\propto 1/c_{low}^2$. As a compromise, all evolutions will be carried out with a lower cutoff of $0.01b$. This will give good results over most of the rapidity range. The value of α_S used will be 0.18, corresponding to a scale of about 10GeV.

Before looking at onium-onium scattering, there are certain properties of the wave function which are worth highlighting.

3.2 The spatial distribution of dipoles

An approximate form for the average dipole distribution has been given in [8]:

$$n(c,b,r,y) \simeq \frac{2b}{cr^2}\log\left(\frac{r^2}{bc}\right)\frac{\exp[(\alpha_{\mathcal{P}}-1)y-\log^2(r^2/bc)/ky]}{(\pi ky)^{3/2}}. \tag{19}$$

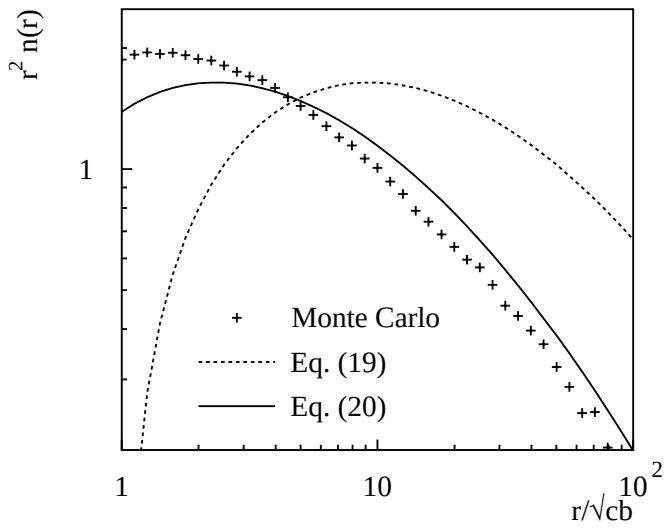

Figure 1: The spatial distribution of dipoles in the onium wave function, for $y = 14$ with $c = b$.

This is the number density of dipoles of size c, at a distance r from the parent dipole of size b, after evolution through a rapidity y. The equation is valid for $r \gg b, c$ and $\log r^2/bc \ll ky$. One of its main characteristics is that the maximum of the dipole distribution is at large r (see the dashed line of figure 1). This would imply that scattering is taking place at values of r where the average dipole distribution would be quite dilute (though fluctuations would still

have to be taken into account). It would also have the consequence that one might reach the dangerous infra-red region, where non-perturbative effects come into play, somewhat sooner than expected. The Monte Carlo results (the + symbols on figure 1), however, show that the distribution is far more central.

The source of this discrepancy is a missing portion of one of the integrals used in the derivation of eq. (19). The details are discussed in Appendix A, where it is shown that a better approximation has an extra factor in the logarithms:

$$n(c,b,r,y) \simeq \frac{2b}{cr^2} \log\left(\frac{16r^2}{bc}\right) \frac{\exp[(\alpha_{\mathcal{P}}-1)y - \log^2(16r^2/bc)/ky]}{(\pi k y)^{3/2}}. \tag{20}$$

This modification also applies to the one-pomeron exchange amplitude, which is why eq. (7) differs from the result derived in [8].

3.3 Localised fluctuations

As already discussed, it is not enough to know just the average distribution of dipoles within the wave function. When calculating multiple pomeron exchange it is necessary to understand the fluctuations. In [10], it was found that there are very significant ($P(n) \propto \exp(-\log^2 n)$) fluctuations in the total number of dipoles of a given size in the onium wave function. The source of these fluctuations is the occasional production of a large dipole which cascades down to give many smaller ones. For multi-pomeron corrections to onium-onium scattering, however, these are not very important, because the dipoles produced from the large dipole will be spread over a large region, giving quite a dilute dipole density. But it was noted that the number of dipoles in a localised region also has significant fluctuations, this time exponential. As is discussed in [8] (and as will be reviewed in section 3.4) an exponential distribution in the dipole density can cause the series for the amplitudes of k-pomeron exchange to be divergent. Therefore these exponential fluctuations warrant more study.

A detailed derivation of the exponential nature of the fluctuations is presented in appendix B. The basis of the derivation is that at very large Y, the c and b dependences factorise, as can be seen from eq. (20). The q^{th} moment of the distribution of dipoles of size c inside a region of size ρ, from a parent of size b which is also in the same region, can then be expressed in the form:

$$n_\rho^{(q)}(c,b,y) = e_q q! A^q(c/\rho) \left(\frac{b}{\rho}\right)^{\nu_q} \mathrm{e}^{q(\alpha_{\mathcal{P}}-1)y}, \tag{21}$$

where, for the purposes of the analysis, A can be any function, though it will actually be proportional to ρ/c. All the moments are defined by the coefficients e_q and the exponents

ν_q which are approximately independent of b. Note that this form explicitly exhibits KNO scaling [11] in c and y. One then obtains the following relations, valid for large q:

$$\nu_q \simeq 2 - \frac{1}{2q\log 2}, \tag{22}$$

and

$$e_q \simeq \frac{1}{4\log 2}\frac{1}{q}\sum_i^{q-i} e_i e_{q-i}\frac{1}{\nu_i + \nu_{q-i} - 2}. \tag{23}$$

Therefore for large q, one has $e_q \propto C^q$, where the exact value of C depends strongly on the behaviour of e_q for low q. This gives for the probability of finding n dipoles of size c within a region of size ρ (in the limit of large n):

$$P_n(c, b, \rho, y) \propto \exp\left[-\frac{n}{A(c/\rho)C\mathrm{e}^{(\alpha_{\mathcal{P}}-1)y}}\right]. \tag{24}$$

This agrees with the Monte Carlo results to within the uncertainties, which are due to the accessible values of y being non-asymptotic and also because the above formulas are valid only for large q, while the value of C retains a dependence on the behaviour of e_q at smaller q.

Note that the shape of the distribution for large n is independent of the size b of the initial dipole: i.e. the shape of the tail of the distribution is independent of the starting conditions of the evolution. For example it is possible to produce high density fluctuations anywhere in impact parameter, as long as a dipole of size $\simeq \rho$ is produced at that point in impact parameter, early on in the evolution, so that it has a long range in y to produce many child dipoles. The only aspect of the tail of the distribution which does depend on the starting conditions is the normalisation: in the above example, the probability of producing a dipole of the appropriate size, at the correct impact parameter, depends on the position and size of the parent dipole.

3.4 Consequences of fluctuations: a toy model calculation

The significance of the exponential density fluctuations is that in [8], Mueller found that exponential fluctuations in a toy model without transverse dimensions led to divergence of the series for the amplitude of k-pomeron exchange. Consider an onium at a rapidity $Y/2$, which has a mean number of dipoles μ ($= \mathrm{e}^{(\alpha_{\mathcal{P}}-1)Y/2}$), with an exponential distribution for the probability of there being n dipoles:

$$P_n(Y/2) \simeq \frac{1}{\mu}\mathrm{e}^{-n/\mu} \tag{25}$$

The amplitude $F^{(k)}$ for the interaction of two onia by exchange of k pomerons is

$$F^{(k)} = \sum_{m,n} \frac{(-\alpha_S^2 mn)^k}{k!} P_m P_n \tag{26}$$

This is valid for $k \ll m, n$. Substituting the exponential probability distributions, and approximating the sum by an integral gives

$$F^{(k)} \sim k!(\alpha_S \mu)^{2k}(-1)^k \tag{27}$$

which for $\alpha_S \mu > 1$ is divergent. The same idea applies in 4 dimensions, as one may see by restricting consideration to the interaction of dipoles of size $c \sim b$ within regions of size b in each onium (this forces all the interactions to take place at roughly the same impact parameter, so that they all contribute to multiple pomeron exchange). These restrictions are appropriate at small impact parameters where the interaction will be dominated by the same region in each onium.

4 Monte Carlo study of onium-onium scattering.

Once one has used a Monte Carlo program to generate a pair onium configurations, as described in section 3, one can go on to look at the interaction between them. This is illustrated in figure 2. The top two plots show typical dipole configurations of two onia. The positions of the initial quark and antiquark are represented by black discs and each 'cigar' shape represents a colour dipole. The evolution in rapidity results in a long chain of dipoles stretching between the quark and anti-quark. The lower left hand plot shows the one-pomeron exchange amplitude as a function of impact parameter (the position of the second onium relative to the first). One can see that the largest interactions occur at an impact parameters where large numbers of dipoles overlap. At impact parameters where no dipoles overlap, there is no interaction. The plot is for a high rapidity ($Y = 20$) and most of the interaction is above 1, and so violates the unitarity limit. The lower right hand plot shows the unitarised amplitude, which is quite flat and close to 1: as one would expect, at large rapidities, the interaction is mostly black.

When determining average amplitudes, two methods have been used. One, as in figure 2, involves determining the interaction at each point of a grid, whose size is chosen to encompass all of the interaction. This gives an estimate of the total interaction for each Monte Carlo event. The second approach is to determine the interaction only along a radial line in impact parameter, from which, after averaging over many events, one can reconstruct the total amplitude. Because one is sampling the onium-onium interaction at fewer points in this

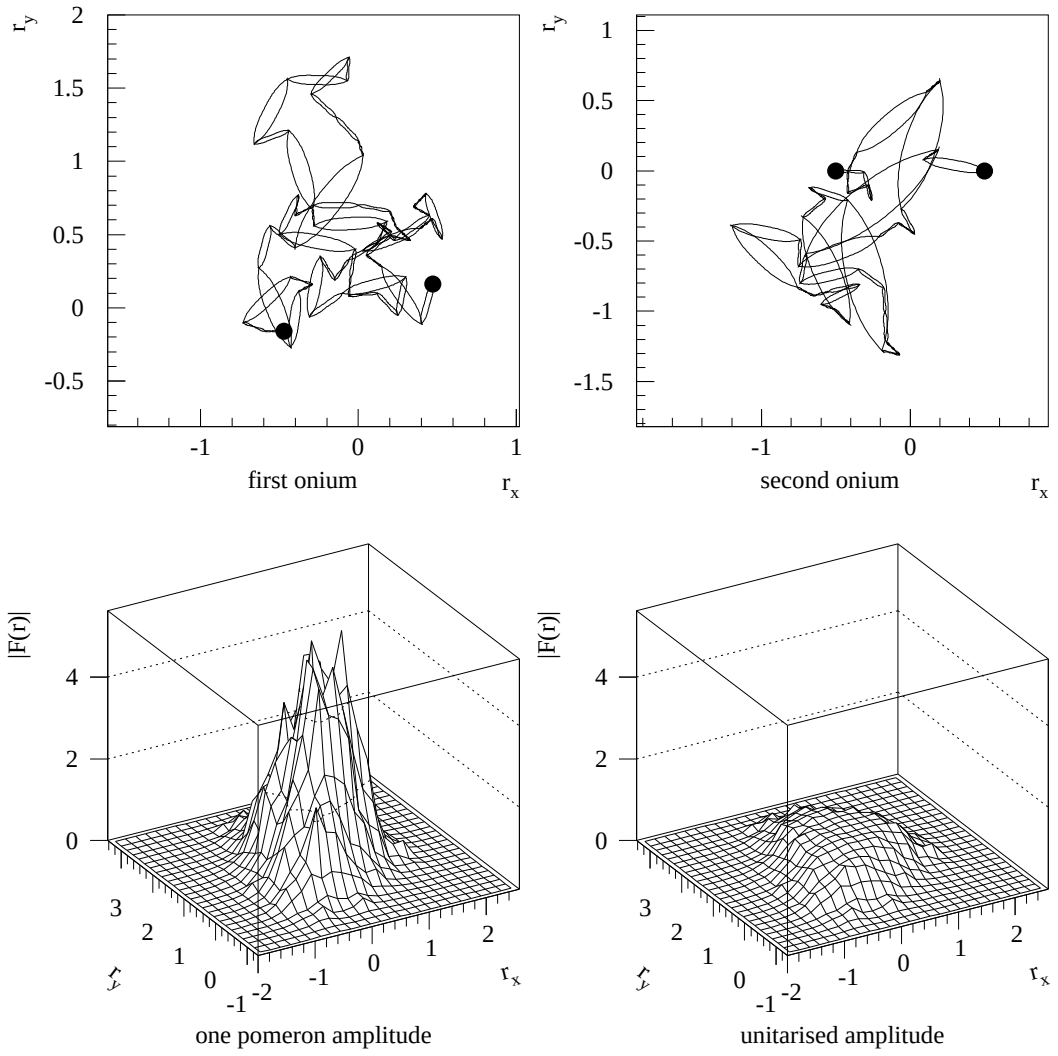

Figure 2: The dipole structure of two onia, each evolved up to rapidity $y = 10$ (each 'cigar' shape represents a dipole). The black discs represent the initial quark and anti-quark. The bottom plots show the amplitude for their interaction as a function of relative impact parameter.

second method, the computational time per pair of configurations is substantially reduced and one can look at a much larger number of configurations. Full details of the Monte Carlo procedure will be presented elsewhere[12].

4.1 1 pomeron, 2 pomeron and unitarised amplitudes

Before drawing any conclusions from the Monte Carlo calculations, it is necessary to check that the answers obtained are in good accord with expectations. All the results which will be given here will be for the collision of onia of the same size, b.

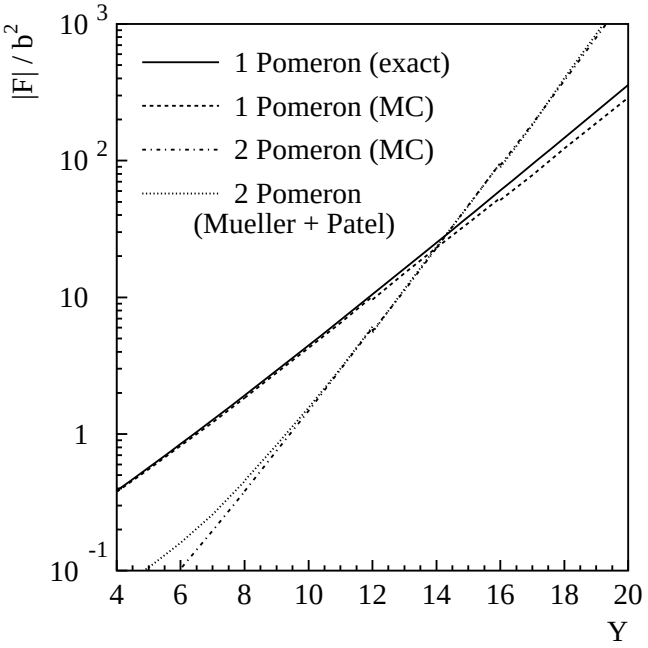

Figure 3: The total amplitude for onium-onium scattering as a function of rapidity. See text for details.

Figure 3 shows Monte Carlo results for 1 pomeron exchange, compared with a result from the numerical solution (as in [10]) of the differential equation governing the evolution [7]. Slight mismatches between Monte Carlo line segments are visible at $Y = 12$ and $Y = 16$: the points between $Y = 12$ and 16 all share the same evolution up to $Y = 12$, so that the errors due to fluctuations in the onium wave function are correlated, making it easier to see the trends in the evolution. The points from $Y = 16$ to 20 share their evolutions up to $Y = 16$, but they use a different set of evolutions from the points $Y = 12 - 16$, hence the mismatch at $Y = 16$ (and analogously at $Y = 12$), which is a measure of the statistical error. Note

that the fluctuations in the wave functions increase at larger Y, while the accessible statistics go down (because of the larger number of dipoles in the onia), so that the statistical error increases at large Y. This is translated into a downwards shift of the amplitude, because one usually misses out on fluctuations with very large amplitudes which would tend to increase the average amplitude. In addition, at higher rapidities a suppression of the same order sets in due to the lower cutoff on dipole size. These small factors aside, the Monte Carlo simulation gives a good estimate of the amplitude.

The main point of figure 3 is to show the relation between the two-pomeron and the one-pomeron amplitudes. This is of interest because the rapidity at which the two amplitudes are the same should be related to the rapidity at which unitarity corrections become important. The cross over occurs at $Y \simeq 14$, corresponding to an energy which is well beyond the reach of current accelerators.

In [7], Mueller and Patel derived the following relation for the total two pomeron amplitude:

$$F^{(2)}(Y) = \lambda \left(\frac{[F^{(1)}(Y)]}{\pi k Y} \right)^2 . \tag{28}$$

The expression which was given for λ was left unevaluated. Eq. (28) is plotted in figure 3, using the Monte Carlo value for $F^{(1)}$, with a fitted value of $\lambda = 6.9 \times 10^2$ (including uncertainties due to the cutoff, there is an error on this of about 5%). The agreement is very good, except at low rapidities where non-asymptotic contributions are important.

The results of sections 3.3 and 3.4 suggest that, beyond the point where one and two pomeron exchange cross over, the k-pomeron exchange series will be divergent and hence of no use in calculating the total cross section. This is clearly visible in figure 4 which shows 1 to 4-pomeron exchange for $Y = 12$–16. Above $Y = 14$ the series looks divergent, while at lower rapidities, it looks asymptotic, with 2 and 3 pomeron exchange crossing over before 1 and 2 pomeron exchange, and so on and so forth for higher k.

One can test the ideas of section 3.4 in more detail by plotting $F^{(k)}(r = 0)/F^{(k-1)}(r = 0)$. In the toy model discussed there, this would be equal to $k(\alpha_S \mu)^2$, giving a straight line when plotted against k (μ was the mean number of dipoles in the onium without transverse dimensions). The same should apply for the case with 2 transverse dimensions, except that $(\alpha_S \mu)^2$ will be replaced by some factor which should be proportional to $F^{(1)}(r = 0)$. The complications due to the transverse dimensions mean that it is not possible to make any prediction about the constant of proportionality.

Figure 5 shows the ratio $F^{(k)}(r = 0)/F^{(k-1)}(r = 0)$ for $Y = 10$. A low value of Y is chosen to allow the greater statistics which are needed to sample the tails of the probability

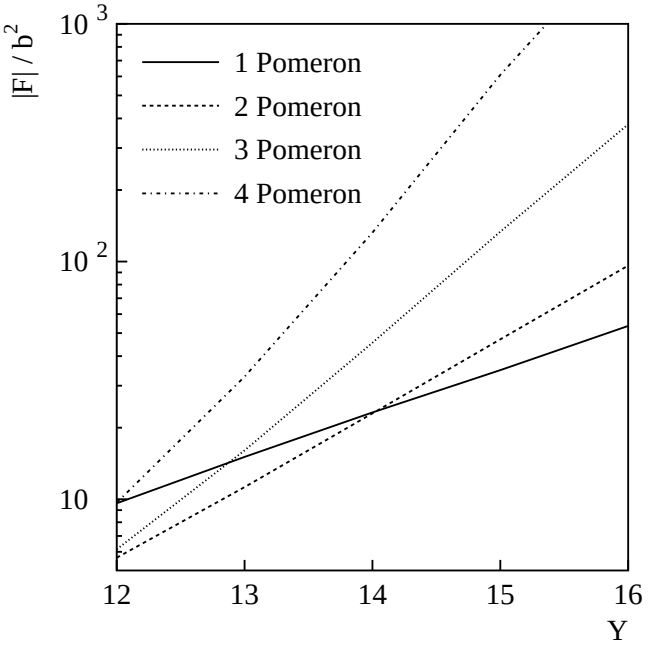

Figure 4: Forward, k-pomeron amplitude for onium-onium scattering as a function of rapidity, as obtained from the Monte Carlo simulation.

distributions, which are relevant for large k. As one can see, the ratio has a clear linear dependence on k. The intercept with the k axis is at non-zero k, indicating that the k pomeron amplitude behaves as $(k+n)!$, rather than $k!$, where $-n \simeq -3$ is the value of the intercept. This difference means that, after taking into account the effects of the transverse dimensions, the fluctuations of the wave functions effectively deviate from exponential at low multiplicities, which is not unreasonable (the calculation showing the fluctuations to be exponential was valid only for the tails of the fluctuations). If one examines plots of the same ratio for other values of Y (in the range $Y = 8$ to 12) one finds that the slope of the straight line is approximately equal to $\beta F^{(1)}(r)$, where $\beta \simeq 0.2$. From the linear dependence of the ratio on k, and the behaviour of its slope with Y, one concludes therefore that the k-pomeron exchange amplitude at $r = 0$ is roughly proportional to $(k+n)![\beta F^{(1)}(0)]^k$, confirming that when unitarisation corrections start to become important, the multiple pomeron series diverges.

So at high rapidities, to understand unitarity corrections it is necessary to use the full unitarised amplitude, resumming multiple pomeron exchange before summing over configurations of the two onia. The results of this are shown in figure 6. Unitarity corrections set in very gradually: even when the amplitude for two pomeron exchange is many times larger

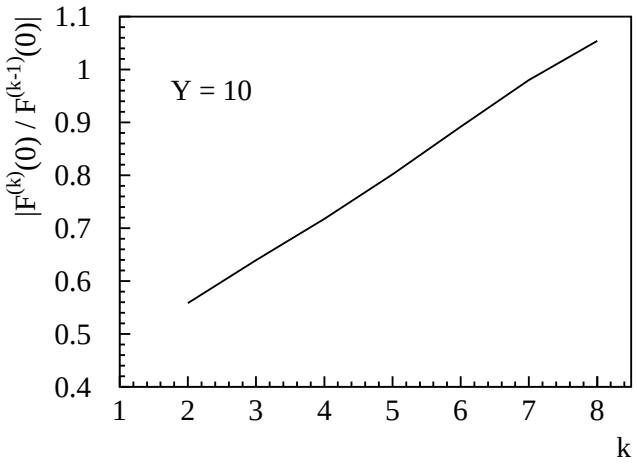

Figure 5: Ratio of k to $(k-1)$-pomeron exchange amplitude for impact parameter $\mathbf{r} = 0$.

than the one pomeron amplitude, the unitarised amplitude carries on growing relatively fast. At a rapidity of $Y \simeq 19$, the reduction in the effective power is only about 25% (see figure 10). The key to understanding why unitarity corrections set in so gradually is in the the profile of the amplitude in impact parameter.

4.2 The profile of the amplitude: $F(r)$.

The profile in impact parameter of the amplitude, $F(r)$, allows one to determine which region contributes most to the cross section, and also which region which has the largest unitarity corrections. The top plot of figure 7 shows $F(r)$ against r. As one would expect, the amplitude is largest at small r and dies off quickly at larger r. However, to understand the contribution to the total amplitude, it is necessary to weight the amplitude with integration area:

$$F = \int \mathrm{d}\log r \; 2\pi r^2 F(r). \tag{29}$$

The lower plot of figure 7 shows the amplitude weighted with r^2, so that the total amplitude is proportional to the area under the curve. The largest contribution to the total amplitude does not come from the region where $F(r)$ is largest: the r^2 enhancement means that radii of the order of 2 or 3 times the parent size are the most important for the total amplitude, even though the average amplitude is considerably smaller there than at $r = 0$.

The two-pomeron amplitude is also shown in figure 7. With increasing r, it dies off faster than the one pomeron amplitude, which means that when weighted with r^2, it is more central.

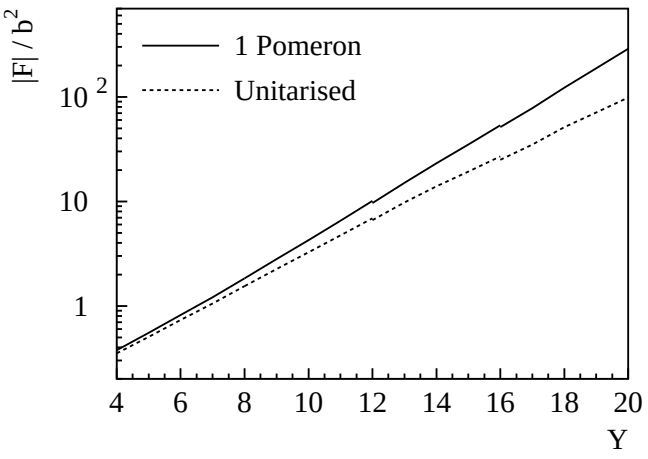

Figure 6: Total 1-pomeron and unitarised onium-onium scattering amplitudes, as obtained from the Monte Carlo simulation.

This is as suggested by Mueller in [8], and the consequence is that the one-pomeron and two-pomeron amplitudes are dominated by different regions of impact parameter: the two-pomeron amplitude can become large without there being large unitarity corrections, because the two-pomeron contribution (and unitarity corrections) grows mostly near $r = 0$, while the total amplitude comes predominantly from larger radii. Note that while $F^{(2)}(r)/F^{(1)}(r)$ decreases with r, the ratio $F^{(2)}(r)/[F^{(1)}(r)]^2$ increases quite rapidly with r, as was predicted in [8] (in fact $F^{(2)}(r)$ decreases even more slowly with increasing r than was suggested there).

Looking again at figure 7, one sees that the largest unitarisation corrections are at also small r, so that the unitarised amplitude, once weighted with r^2, has its maximum at larger r than the one pomeron amplitude. However, the unitarised amplitude is still considerably suppressed (compared to the one pomeron amplitude), even at radii where $F^{(1)}(r) \ll 1$. This is indicative of large fluctuations, or alternatively that eikonalisation is a poor approximation (and is also related to the strong rise in the ratio $F^{(2)}(r)/[F^{(1)}(r)]^2$ with increasing r). The eikonal approximation is valid in the limit of no fluctuations: if $F^{(1)}(\mathbf{r})$ is the same for each event then unitarisation can be done after averaging over events:

$$-F^{unit}(r) \simeq -F^{eik}(r) = 1 - e^{F^{(1)}(r)}, \tag{30}$$

bearing in mind that $F^{(1)}$ is negative. Figure 8 shows the ratios $F^{unit}/F^{(1)}$ and $F^{eik}/F^{(1)}$. For very small r where the amplitude is quite black, the eikonalised and unitarised amplitudes

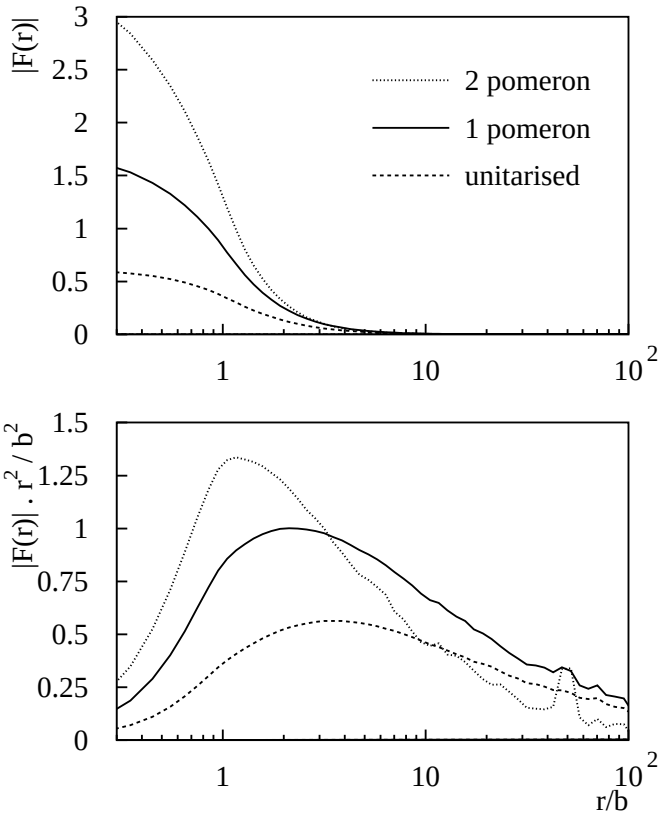

Figure 7: The top plot shows the average amplitude as a function of r. In the lower plot, the amplitude is weighted with r^2 so that the area under the curve is proportional to the cross section. $Y = 14$.

are both strongly reduced, and to a similar extent. They do differ slightly, and this is the form of failure of eikonalisation found in the toy model [8]. However if one examines the radii which contribute most to the total amplitude ($r \simeq 2b \to 3b$), eikonalisation would predict only very small corrections, whereas the unitarised cross section is reduced by a factor of two roughly, compared to the one pomeron value. This means that the configurations contributing most to the one-pomeron cross section actually have relatively large amplitudes. Therefore for the average amplitude to still be low, the one-pomeron amplitude must be dominated by rare configurations.

The lower plot of figure 8 shows that this is in fact the case. The solid curve is the probability distribution of the amplitude $F^{(1)}(\mathbf{r})$ for $|\mathbf{r}| = 2b$. The dashed curve shows this probability distribution weighted by $F^{(1)}(r)$, normalised so that the total area under

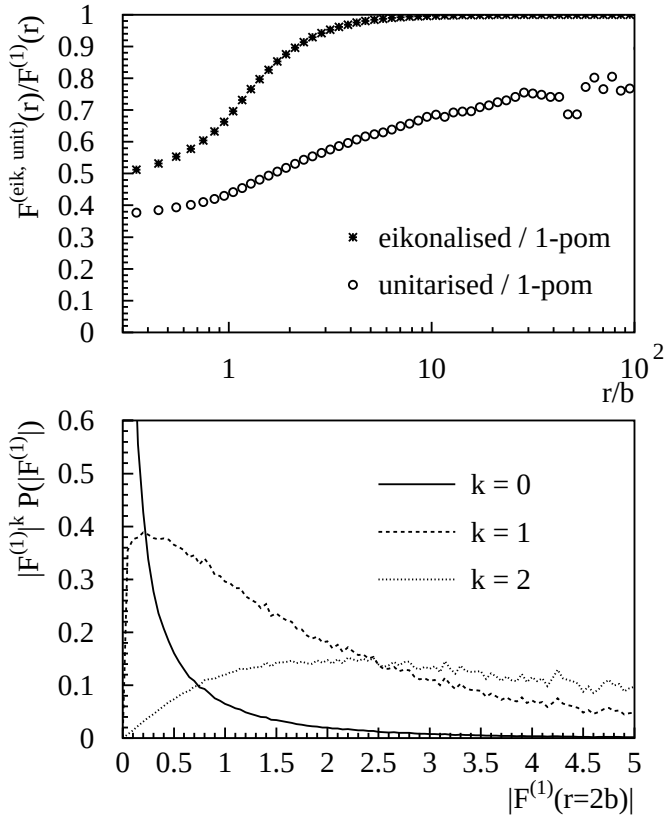

Figure 8: Top plot: the ratio of the unitarised and eikonalised to the one pomeron amplitude, as a function of r. Bottom plot: the probability distribution of $F^{(1)}$ for a fixed impact parameter, $|\mathbf{r}| = 2b$. Both plots are for $Y = 14$

it is 1. The area under a particular region of the curve is indicative of how much that region contributes to the average amplitude at $\mathbf{r}$. The unweighted distribution is very sharply peaked at $F^{(1)} = 0$. Yet the weighted distribution is spread over a wide range of $F^{(1)}$: 80% of the amplitude comes from from only 10% of the configurations. This is at the value of r which contributes most to the total amplitude. There is also a contrast between the curves for 1 pomeron and 2 pomeron (i.e. weighted with $[F^{(1)}]^2(r)$) exchange, however it is less marked: the region contributing 80% to the two pomeron amplitude contributes 40% to the one pomeron amplitude, though this region comes from only 2.5% of configurations, so that the two-pomeron amplitude here is dominated by somewhat rarer configurations than the one-pomeron amplitude. The same phenomenon, of rare configurations dominating one and multi-pomeron exchange is even more accentuated at larger r. It is also worth pointing out

that since the total amplitude comes mostly from moderate values of r, it too is dominated by large fluctuations: at $Y = 14$, two thirds of the total one-pomeron amplitude comes from only 10% of events.

The main reason why the amplitude at a given impact parameter is dominated by such a small fraction of configurations is that for an impact parameter somewhat away from the onium, dipoles are most likely to be first produced there later on in the evolution. But if they appear there only late then they won't have a sufficient rapidity range to build up in numbers. However if a dipole is produced there early on (an unlikely occurrence) then it will cascade into many dipoles and give a large interaction. These rare, (and at larger Y, strongly unitarised) configurations dominate the amplitude, so that even though the amplitude will on average be small, it can have significant unitarity corrections. In addition these rare configurations will not have circular symmetry, so that even when a state of size r is produced, a point $\mathbf{r}$ will only have an interaction if the orientations of the configurations are appropriate, further increasing the fluctuations in the amplitude at a given point.

What allows the amplitude to continue growing at large rapidities, is that, for any given impact parameter, the probability of the configurations with large interactions can carry on increasing until they become common. But there will always be larger radii at which large interactions are not yet common, so that the total amplitude can carry on increasing through an effective increase in the total area of interaction. This ignores of course the effect of saturation of the wave function, or confinement effects placing a maximum limit on the dipole size.

4.3 Elastic scattering

The unitarity corrections to the total amplitude (and correspondingly, total cross section) set in quite slowly, because the increase in the effective area of interaction allows the total cross section to carry on rising. However the amplitude is strongly unitarised at small impact parameters, and concentrating on this region should make it much easier to see the onset of unitarity. A crude way of doing this is to look at the elastic onium-onium cross section. An expression for the differential elastic cross section was given in eq. (5), but it is best to look initially at the integrated elastic cross section which can be written:

$$\sigma_{el} = \int \mathrm{d}^2\mathbf{r} |A(\mathbf{r}, Y)|^2 \tag{31}$$

One should remember that $A(\mathbf{r}, Y)$ is obtained from $F(\mathbf{b}, \mathbf{b}', \mathbf{r}, Y)$ by integrating over $\mathbf{b}$ and $\mathbf{b}'$ in the $q\bar{q}$ component of the wave functions of the two onia. However, for the purpose of understanding the essentials of the behaviour of the elastic cross section, this complication

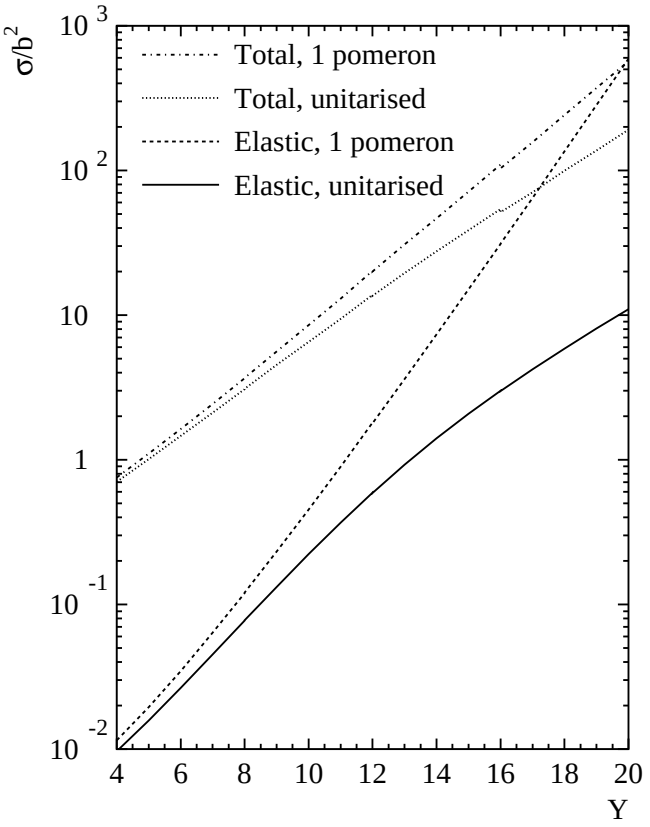

Figure 9: The elastic and total cross sections for onium-onium scattering, as a function of rapidity, showing both the one-pomeron approximation and the fully unitarised results.

will be ignored: $|F|$ will be used instead of $|A|$. The leading power behaviour of F is $1/r^2$, which is why for the total cross section, large impact parameters can contribute. For the elastic cross section, though, one is integrating the square of the amplitude, which will fall off as $1/r^4$. So the integral is dominated by small r, where the unitarisation is strongest. Another aspect of the problem, is that the elastic cross section can't exceed half the total cross section (the unitarity condition), but the asymptotic power growth with Y of the elastic cross section (in the one pomeron approximation) is twice that of the total cross section. Therefore unitarisation must reduce the power growth of the elastic cross section by more than a factor of two.

Figure 9 shows the one pomeron and unitarised calculations for the elastic cross section, together with the analogous results for the total cross sections, for reference. As suggested, the unitarisation corrections to the elastic cross section are much larger than those to the total

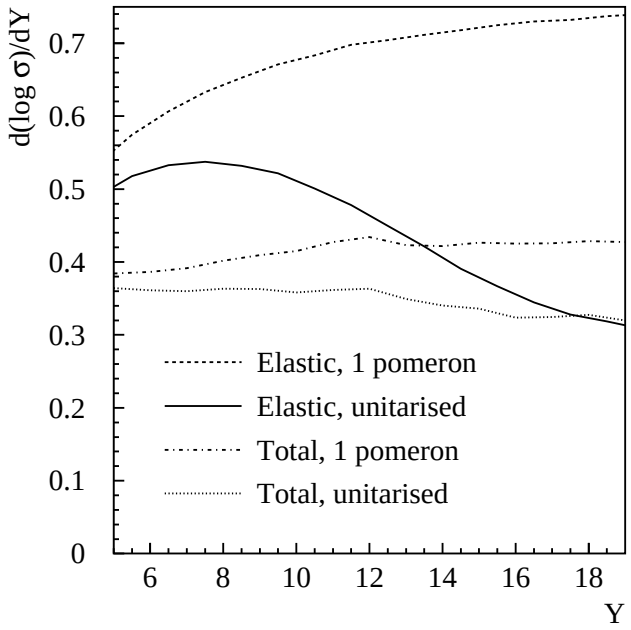

Figure 10: The power dependence in rapidity of the total and elastic, 1-pomeron and unitarised cross sections, as a function of rapidity.

cross section, and one clearly sees the rate of increase of the elastic cross section tailing off to take the same value as that of the total cross section. One also sees that at large rapidity, the fraction of the total cross section which comes from elastic scattering is relatively small (about 0.06), certainly well below the unitarity bound of 1/2. The reason for this is, again, that the total cross section is coming from a large region in impact parameter where the amplitude is small, and so does not contribute much to the elastic cross section. It is also worth briefly noting, in view of the discussion on eikonalisation in the previous section, that the rapidity where the one-pomeron total and elastic cross sections cross over ($Y \simeq 20$), is the same as the point where the one and two pomeron contributions to the total cross section would cross if the eikonal approximation were valid.

In figure 10, the effective power dependence of the total and elastic cross sections is plotted against Y. Looking first at the 1 pomeron cross sections, one sees that they vary with Y, tending only relatively slowly to their asymptotic values of 0.47 and 0.94 respectively. This is a result of the logarithmic corrections which are $1/\sqrt{Y}$ and $1/Y^3$ for the total and elastic cross sections. The power for the unitarised total cross section deviates only slowly from the 1-pomeron power, and its variation with Y is also slow. The unitarised elastic cross section, on

the other hand, grows with a power which differs quite noticeably from the 1-pomeron elastic cross section, and the variation of the power with Y is also very different, decreasing rather than increasing from $Y = 8$ onwards, tending towards the same power as the unitarised total cross section at large rapidity. This significant decrease in the elastic power, if not masked by other effects, might be a clear signal for the onset of unitarity corrections.

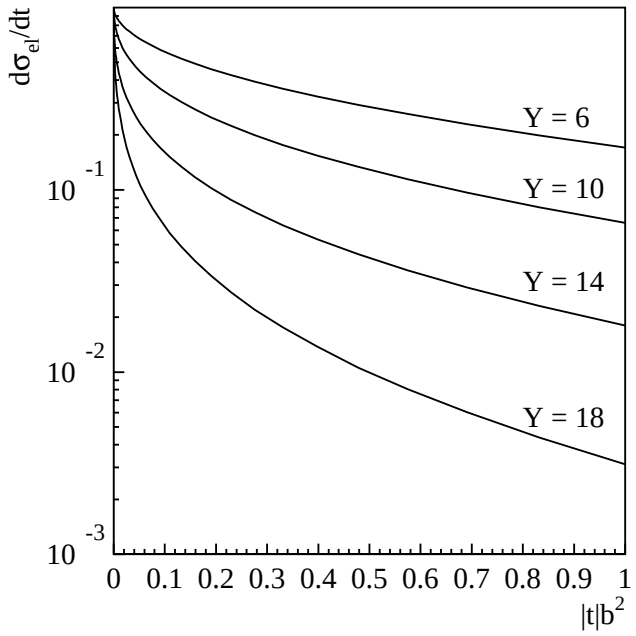

Figure 11: The unitarised differential elastic cross section for different values of Y.

Finally, for completeness, it is worth looking at the differential elastic cross section, figure 11, as a function of the square of the exchanged momentum, t. It is very strongly peaked at $t = 0$, because in impact parameter the amplitude dies off so slowly at large r. As Y increases, the region of interaction gets larger, which causes the elastic peak to become narrower in t.

5 Conclusions

By performing a Monte Carlo simulation of the dipole formulation of onium-onium elastic scattering, it has been possible to calculate single and multi-pomeron scattering amplitudes as a function of rapidity and impact parameter. The energy where one and two pomeron total amplitudes are comparable, has been determined to be $Y \simeq \log s/M^2 \simeq 14$ (with

$\alpha_S = 0.18$). However, the multiple pomeron series is not a very good way of calculating unitarity corrections. There are two reasons for this. Firstly, the multiple pomeron series diverges. This is a consequence of the dipole density in an onium wave function having exponential fluctuations. For multiple pomeron exchange, the enhancement due to multiple coupling to these very dense configurations more than compensates for their low probability. This necessitates the resummation of all numbers of pomeron exchange before averaging over onium configurations. Nevertheless, one might have expected that once, say, two pomeron exchange became larger than one pomeron exchange, the unitarised amplitude would quickly stop growing. It doesn't: unitarity corrections set in very slowly, with the correction to the effective power of the growth being only of the order of 25%, even at a rapidity of $Y = 19$.

The main reason for this is that the growth of the total multiple pomeron amplitude is due mostly to an increase in the interaction at central impact parameters. The unitarised amplitude, on the other hand effectively carries on growing through an increase in the area of interaction, even when it has already reached the unitarity bound at a given point in impact parameter. This though is still a simplification. One finds that the impact parameters contributing most to the total amplitude have low average amplitudes, yet significant unitarity corrections. In fact, the average amplitude there is dominated by rare configurations with large amplitudes and large unitarity corrections: the growth of the total amplitude comes through an increase in the probability of these rare configurations.

Since the unitarisation is largest at small impact parameters, it is useful to find a process where small impact parameters matter more. Elastic scattering has this property because it depends on the square of the average amplitude so regions with the largest amplitudes (and strongest unitarisation) contribute most. One finds that the unitarisation effects start to become important as early as $Y = 8$: the one-pomeron approximation to $\mathrm{d}\log\sigma_{el}/\mathrm{d}t$ carries on increasing with Y, while the unitarised power starts to decrease.

There are a number of difficulties when trying to relate these results to experimentally feasible measurements. Ideally one would want to examine a process such as that suggested by Mueller and Navelet [13], where the BFKL evolution occurs between two objects with similar, large, transverse scales. However, the evidence currently for BFKL type behaviour is in results from HERA, both in the measurement of the rise of the structure function F_2 at small x [14, 15] (analogous to a total cross section) and more recently from the rise (roughly twice as fast) of the elastic electro-production of ρ^0 and J/ψ and elastic photo-production of J/ψ [16, 17, 18, 19, 20] (analogous to elastic scattering). Complications arise in trying to understand the unitarity corrections in these types of processes, partly because the evolution is taking place over a range of scales, but also because of the non-perturbative effects associated

with the proton scale. In particular, these would prevent the large size fluctuations, which are so important for the continued growth of the BFKL total cross section beyond the point where unitarisation becomes significant.

Acknowledgements

I am very grateful to A.H. Mueller and B.R. Webber for many helpful conversations and for suggesting this work, as well as to M. Diehl, F. Hautmann, R. Peschanski and W.-K. Tang for useful discussions.

Appendix A: The mean spatial distribution of dipoles.

The discrepancy between the Monte Carlo results for the dipole distribution and the analytical prediction from Mueller [8] is related to the details of one of the integrals involved in its evaluation. In determining eq. (19) one goes through the following stage:

$$n(c,b,r,y) = \int \frac{\mathrm{d}\nu}{2\pi} H_\nu(\mathbf{c},\mathbf{b},\mathbf{r}) \frac{b}{c} \exp\left[\frac{2\alpha_S N_C}{\pi}\chi(1+2i\nu)y\right] \tag{32}$$

where

$$H_\nu(\mathbf{c},\mathbf{b},\mathbf{r}) = \frac{4\nu^2}{\pi^2} b^{-2i\nu} c^{2i\nu} \int \frac{\mathrm{d}^2\mathbf{R}}{[|\mathbf{R}-\mathbf{b}/2||\mathbf{R}+\mathbf{b}/2|]^{1-2i\nu}[|\mathbf{R}+\mathbf{r}-\mathbf{c}/2||\mathbf{R}+\mathbf{r}+\mathbf{c}/2|]^{1+2i\nu}} \tag{33}$$

The BFKL characteristic function, $\chi(\gamma)$, is

$$\chi(\gamma) = \psi(1) - \frac{1}{2}\psi(1-\gamma/2) - \frac{1}{2}\psi(\gamma/2), \tag{34}$$

where ψ is the digamma function. First, cut out the regions $R < Pb$ and $|\mathbf{R}+\mathbf{r}| < Pc$, where P is an arbitrary constant satisfying $P \gg 1$ and $4\nu P \ll 1$. The integral without these regions gives:

$$\frac{2i\nu}{\pi r^2}\left[\left(\frac{r^2}{P^2 bc}\right)^{-2i\nu} - \left(\frac{r^2}{P^2 bc}\right)^{2i\nu}\right]. \tag{35}$$

One can see, by taking the limit $\nu \to 0$, that there should be no terms of order ν within the square bracket, because the integral is similar to the one evaluated in [6] for the virtual corrections to the dipole kernel. The result obtained in [8] is equivalent to taking $P = 1$ and neglecting other contributions. Now consider one of the regions that was cut out. It can be integrated as follows:

$$\frac{4\nu^2}{\pi^2}\frac{b^{-2i\nu}c^{2i\nu}}{r^{2+4i\nu}} \int^{R<Pb} \frac{R\mathrm{d}R\mathrm{d}\theta}{(R\sqrt{b^2-2bR\cos\theta+R^2})^{1-2i\nu}} \tag{36}$$

$$\simeq \frac{4\nu^2}{\pi^2}\frac{(P^2bc)^{2i\nu}}{r^{2+4i\nu}} \int^{R<Pb} \frac{\mathrm{d}R\mathrm{d}\theta}{\sqrt{b^2-2bR\cos\theta+R^2}}. \tag{37}$$

The approximation giving the second line is valid because of the condition $\nu P \ll 1$, so that in the range of R important for the integration, the power ν has little effect on the value of the integrand. The angular integral can be performed to give a complete elliptic integral of the first kind, $[4\mathbf{K}(R/b)/b]$ for $R < b$ and $[4\mathbf{K}(b/R)/R]$ for $R > b$ [21]. Performing the R integral then gives

$$\frac{8\nu^2}{\pi r^2}\left(\frac{r^2}{P^2bc}\right)^{-2i\nu}\left[\log 4P + O(\nu)\right] \simeq \frac{2i\nu}{\pi r^2}\left(\frac{r^2}{P^2bc}\right)^{-2i\nu}\left[(16P^2)^{-2i\nu} - 1 + O(\nu^2)\right]. \qquad (38)$$

Adding this, and a similar term for the dipole of size c, to eq. (35) gives

$$H_\nu(\mathbf{c},\mathbf{b},\mathbf{r}) \simeq \frac{2i\nu}{\pi r^2}\left[\left(\frac{16r^2}{bc}\right)^{-2i\nu} - \left(\frac{16r^2}{bc}\right)^{2i\nu}\right]. \qquad (39)$$

Following through the calculation, gives for the dipole density:

$$n(c,b,r,y) = \frac{2b}{cr^2}\log\left(\frac{16r^2}{bc}\right)\frac{\exp[(\alpha_{\mathcal{P}}-1)y - \log^2(16r^2/bc)/ky]}{(\pi ky)^{3/2}}. \qquad (40)$$

This is much more central and agrees well with the Monte Carlo distributions.

Appendix B: Fluctuations in the localised dipole number

The approach used, will be to study the equations for the moments of the dipole distribution within a region of radius ρ. The first step is to note that branching sequences that include dipoles of sizes larger than ρ will not contribute to high density fluctuations: the number dipoles of size ρ coming from a dipole of size $R \gg \rho$ will be at most enhanced by a factor proportional to R/ρ (just the usual factor in front of the BFKL saddle point solution). However dipoles will be spread out over a region of size R^2, so that the density of dipoles will be suppressed by a factor ρ/R. Therefore in calculations one can leave out all dipoles larger than ρ. One can also neglect the transverse positions of the dipoles, since, if a dipole starts inside a region of size ρ, and the branching involves no dipoles larger than ρ, most of the child dipoles will still be inside the region.

Define $n_\rho^{(q)}(c,b,y)$ to be the q^{th} moment of the number of dipoles of size c in a region of radius ρ originating from a parent of size b after an evolution through rapidity y. (The q^{th} moment being $\langle n(n-1)\dots(n-q+1)\rangle$). It will then approximately satisfy the following equation:

$$\frac{\mathrm{d}n_\rho^{(q)}(c,b,y)}{\mathrm{d}y} = I_\rho^{(q)} + \frac{\alpha_S N_C}{2\pi^2}\int^\rho \frac{b^2\mathrm{d}^2\mathbf{b}_2}{b_{02}^2 b_{12}^2}\left[n_\rho^{(q)}(c,b_{02},y) + n_\rho^{(q)}(c,b_{12},y) - n_\rho^{(q)}(c,b_{01},y)\right]. \qquad (41)$$

The inhomogeneous term, $I_\rho^{(q)}$, is

$$I_\rho^{(q)} = \frac{\alpha_S N_C}{2\pi^2}\int^\rho \frac{b^2\mathrm{d}^2\mathbf{b}_2}{b_{02}^2 b_{12}^2}\sum_{i=1}^{q-1} C_i^q n_\rho^{(i)}(c,b_{02},y) n_\rho^{(q-i)}(c,b_{12},y) \qquad (42)$$

This is obtained from the generating functional equation in [6], with an upper cutoff placed on the dipole size in the $\mathbf{b}_2$ integration.

The first approximation to make relies on the large Y limit. At large Y, with c and b not too different, one has for the total average number of dipoles:

$$n(c,b,Y) \propto \frac{b}{c} \mathrm{e}^{(\alpha_{\mathcal{P}}-1)Y} \tag{43}$$

The important point is that the b dependence (which shows a power behaviour) factors out from the c and Y dependences. This will apply to the moments of the localised dipole distribution as well. It will further be useful to make the assumption (reasonably justifiable) that the b dependences of the moments are also power behaviours. One can then parameterise each moment by two constants e_q and ν_q, which should depend only weakly on b:

$$n_{\rho}^{(q)}(c,b,Y) = e_q q! A^q(c/\rho) \left(\frac{b}{\rho}\right)^{\nu_q} \mathrm{e}^{q(\alpha_{\mathcal{P}}-1)Y}. \tag{44}$$

It is not necessary to know the exact c dependence, which is why it is left as $A(c)$. With this parameterisation, eq. (41) can be written as:

$$q(\alpha_{\mathcal{P}}-1)\left(\frac{b}{\rho}\right)^{\nu_q} e_q = \frac{\alpha_S N_C}{\pi}\left[k_{\nu_q}\left(\frac{b}{\rho}\right)^{\nu_q} e_q + \left(\frac{b}{\rho}\right)^2 \sum_{i=1}^{q-1} e_i e_{q-i} l_{\nu_i \nu_{q-i}}\right]. \tag{45}$$

The following integrals have been defined:

$$k_\nu = \frac{1}{2\pi}\left(\frac{b}{\rho}\right)^{-\nu} \int^{\rho} \frac{b^2 \mathrm{d}^2 b_2}{b_{02}^2 b_{12}^2}\left[\left(\frac{b_{02}}{\rho}\right)^{\nu} + \left(\frac{b_{12}}{\rho}\right)^{\nu} - \left(\frac{b}{\rho}\right)^{\nu}\right], \tag{46}$$

and

$$l_{\nu\nu'} = \frac{1}{2\pi}\left(\frac{b}{\rho}\right)^{-2} \int^{\rho} \frac{b^2 \mathrm{d}^2 b_2}{b_{02}^2 b_{12}^2}\left[\left(\frac{b_{02}}{\rho}\right)^{\nu}\left(\frac{b_{12}}{\rho}\right)^{\nu'}\right]. \tag{47}$$

For $1 \leq \nu < 2$ (as should be the case for all q), k_ν and $l_{\nu\nu'}$ will depend only weakly on b/r (except for l_{11} which has a logarithmic dependence on b/r — this is discussed later).

The main difference between the two terms is that the $l_{\nu\nu'}$ integral is dominated by large $b_2 \sim \rho$, while the k_ν integral, because of the condition given above on ν, the integral is dominated by small $b_2 \sim b$. This is the origin of the different power behaviours from the two integrals.

To solve eq. (45) one uses the fact that $\nu_q < 2$, therefore for large ρ/b the inhomogeneous term drops out, leaving:

$$q(\alpha_{\mathcal{P}}-1) \simeq \frac{\alpha_S N_C}{\pi} k_{\nu_q}. \tag{48}$$

Through the ν dependence in k_ν, this fixes ν_q. For moderately large q, k_ν can be approximated as

$$k_\nu \simeq \frac{2}{2-\nu} \tag{49}$$

giving

$$\nu_q = 2 - \frac{1}{2q\log 2} \tag{50}$$

Note that this is just the solution to the equation $\chi(\nu) = q\chi(1)$, in the limit $\nu \to 2$, with χ defined as in eq. (34). The other region which can be studied to help solve eq. (45) is that of b close to ρ. For the case of ν close to 2, i.e. for large q, at large b, the integral for k_ν is much smaller than its asymptotic value (it only reaches its asymptotic value for $\rho/b \sim \exp[1/(2-\nu)]$), while that for $l_{\nu\nu'}$ should be much closer to its asymptotic value (the integrand is approximately proportional to b_2). Therefore the k_ν term can be neglected, giving

$$e_q \simeq \frac{1}{4\log 2}\frac{1}{q}\sum_i^{q-i} e_i e_{q-i} l_{\nu_i \nu_{q-i}} \tag{51}$$

A reasonable approximation for $l_{\nu_1\nu_2}$ is:

$$l_{\nu\nu'} \simeq \frac{1}{\nu+\nu'-2}. \tag{52}$$

By iterating eq. (51), one can determine all the moments of the fluctuations. Its form is such that for large q, e_q should be behave as follows:

$$e_q \simeq BC^q \tag{53}$$

Because of the complicated behaviour of the coefficients of the iteration for low values of q, it is not possible to provide an analytical approximation for B and C, though they can be determined numerically. This then gives an exponential distribution for the fluctuations in dipole number in a restricted region, $\mathrm{e}^{-n/\mu}$ where

$$\mu(c/r) = A(c/r)Ce^{(\alpha_{\mathcal{P}}-1)Y} \tag{54}$$

It is difficult to compare this directly with the results from the Monte Carlo simulation, because $A(c/r)$ contains various logarithmic factors which are difficult to estimate accurately. However the mean number of dipoles of a given size in a certain region is something that can be obtained from the Monte Carlo distribution and so $A(c/\rho)$ can be factored out:

$$\frac{\mu(c/\rho)}{n_\rho(c,\rho,Y)} \simeq C \simeq \lim_{q\to\infty} \frac{e_q}{e_{q-1}}. \tag{55}$$

In evaluating C from the recursion relations there are some complications because the first relation contains l_{11} which varies logarithmically with b/ρ (this is the reason why the expression given in eq. (52) diverges). Given that the values of e_q are determined by the region of b close to ρ, it is then natural to use a value of l_{11} corresponding also that region of b. For $b = 0.5\rho$, $l_{11} = 1.9$ (determined numerically), while for $b = 0.25\rho$, $l_{11} = 2.7$. This range will be used when calculating the e_q to gauge the uncertainty in the calculation.

Another uncertainty arises because at the rapidities available to the Monte Carlo simulation, the logarithmic prefactors affect the effective power growth of the distribution. To gauge this effect, one can replace $(\alpha_{\mathcal{P}} - 1)$ with a measured effective power and look at the difference that this makes to C. The final range of values obtained for C is from 0.34 to 0.75.

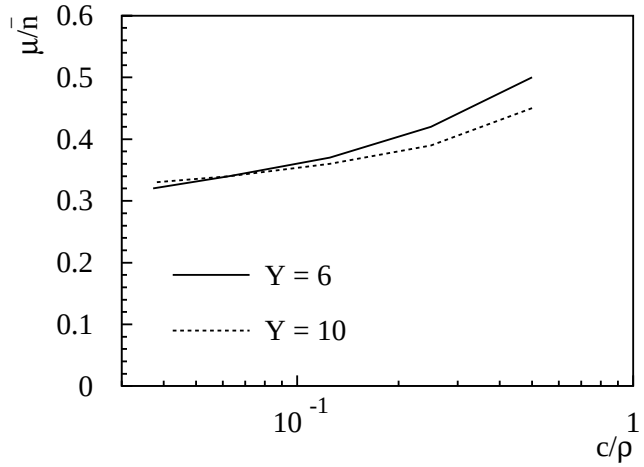

Figure 12: The parameter C of eq. (55), as determined by Monte Carlo simulation for two values of y.

Figure 12 shows the value of $C_{MC} = \mu(c/\rho)/[2n_\rho(c,\rho/2,Y)]$ determined from the Monte Carlo simulation for two values of Y and a range of c/ρ. The values for C from the iteration of eq. (51) are consistent with the Monte Carlo results. However the Monte Carlo results do depend slightly on Y and on c/ρ. For the variation with Y at $c \sim \rho$, C_{MC} decreases as Y increases. This could be because at larger Y, the effective power is larger. A larger effective power leads to a reduced value for e_q/e_{q-1} (this can be seen by making some simple analytic approximations, and is also obtained in the numerical iterations). A second effect is that

at smaller c/ρ, the presence, non-asymptotically, of factors of the form $\exp[-\log^2(c/\rho)/kY]$ leads to an increase in the effective power with decreasing c, giving a decreasing C. At larger Y this effect would be smaller, so, at larger Y, C should decrease more slowly with decreasing c. Both of these observations are qualitatively in accord with the Monte Carlo results.

References

[1] Y. Y. Balitskiĭ and L. N. Lipatov, Sov. Phys. JETP **28**, 822 (1978).

[2] E. A. Kuraev, L. N. Lipatov, and V. S. Fadin, Sov. Phys. JETP **45**, 199 (1977).

[3] L. N. Lipatov, Sov. Phys. JETP **63**, 904 (1986).

[4] J. Kwieciński, A. D. Martin, and P. J. Sutton, Phys. Rev. **D44**, 2640 (1991).

[5] L. V. Gribov, E. M. Levin, and M. G. Ryskin, Phys. Rep. **100**, 1 (1983).

[6] A. H. Mueller, Nucl. Phys. **B415**, 373 (1994).

[7] A. H. Mueller and B. Patel, Nucl. Phys. **B425**, 471 (1994).

[8] A. H. Mueller, Nucl. Phys. **B437**, 107 (1995).

[9] Z. Chen and A. H. Mueller, Columbia preprint CU-TP-691 (1995).

[10] G. P. Salam, Nucl. Phys. **B449**, 589 (1995).

[11] Z. Koba, H. B. Nielsen, and P. Olesen, Nucl. Phys. **40**, 317 (1972).

[12] G. P. Salam, Cavendish preprint HEP-95/07, in preparation. (1995).

[13] A. H. Mueller and H. Navelet, Nucl. Phys. **B282**, 727 (1987).

[14] H1 Collaboration, DESY 95-006 (1995).

[15] J.I. Fleck on behalf of the ZEUS Collaboration, GLAS-PPE/95-01 (1995).

[16] ZEUS Collaboration, DESY 95-133 (1995).

[17] ZEUS Collaboration, DESY 95-052 (1995).

[18] H1 Collaboration, Submission to Brussels EPS Conference, EPS-0490 (1995).

[19] H1 Collaboration, Submission to Brussels EPS Conference, EPS-0468 (1995).

[20] H1 Collaboration, Submission to Brussels EPS Conference, EPS-0469 (1995).

[21] I. S. Gradshteyn and I. M. Ryzhik, *Table of Integrals, Series and Products*, Academic Press, 1965.